

This article was downloaded by:

On: 19 January 2011

Access details: *Access Details: Free Access*

Publisher *Taylor & Francis*

Informa Ltd Registered in England and Wales Registered Number: 1072954 Registered office: Mortimer House, 37-41 Mortimer Street, London W1T 3JH, UK



## International Journal of Polymeric Materials

Publication details, including instructions for authors and subscription information:

<http://www.informaworld.com/smpp/title~content=t713647664>

### Monitoring the Evolution of Morphology of Polymer Blends Upon Manufacturing of Microfibrillar Reinforced Composites

J. A. Covas<sup>a</sup>; O. S. Carneiro<sup>a</sup>; J. M. Maia<sup>a</sup>

<sup>a</sup> Department of Polymer Engineering, University of Minho, Guimarães, Portugal

**To cite this Article** Covas, J. A. , Carneiro, O. S. and Maia, J. M.(2011) 'Monitoring the Evolution of Morphology of Polymer Blends Upon Manufacturing of Microfibrillar Reinforced Composites', *International Journal of Polymeric Materials*, 50: 3, 445 – 467

**To link to this Article:** DOI: 10.1080/00914030108035119

**URL:** <http://dx.doi.org/10.1080/00914030108035119>

PLEASE SCROLL DOWN FOR ARTICLE

Full terms and conditions of use: <http://www.informaworld.com/terms-and-conditions-of-access.pdf>

This article may be used for research, teaching and private study purposes. Any substantial or systematic reproduction, re-distribution, re-selling, loan or sub-licensing, systematic supply or distribution in any form to anyone is expressly forbidden.

The publisher does not give any warranty express or implied or make any representation that the contents will be complete or accurate or up to date. The accuracy of any instructions, formulae and drug doses should be independently verified with primary sources. The publisher shall not be liable for any loss, actions, claims, proceedings, demand or costs or damages whatsoever or howsoever caused arising directly or indirectly in connection with or arising out of the use of this material.

# Monitoring the Evolution of Morphology of Polymer Blends Upon Manufacturing of Microfibrillar Reinforced Composites

J. A. COVAS\*, O. S. CARNEIRO† and J. M. MAIA‡

*Department of Polymer Engineering, University of Minho,  
Campus de Azurém, 4800 Guimarães, Portugal*

*(Received 14 February 2001; In final form 20 February 2001)*

Microfibrillar reinforced composites (MFC) based on HDPE/PET blends were prepared under conditions relevant for direct scale-up to an industrial process. The evolution of the morphology and of the linear viscoelastic response of the blend along the axis of a co-rotating twin screw extruder and at several locations along the extrusion line was monitored. Major changes in the average particle size and size distribution of the disperse phase occurred upon melting of the components, whilst a much slower evolution rate was evident downstream in the extruder. Simultaneously,  $G'$  and  $G''$  increased along the extruder. Pellets showing well oriented PET fibrils embedded in a HDPE matrix with poor adhesion between both were obtained. This MFC showed the typical improvement expected in mechanical performance when compared with the matrix.

*Keywords:* Microfibrillar reinforced composites; Polymer blends; Morphology; Rheology

## 1. INTRODUCTION

Research efforts to yield new plastic materials with improved performance have been developed along various routes, among them

---

\* Corresponding author. Tel.: 351253510245, Fax: 351253510249, e-mail: jcovas@dep.uminho.pt

† e-mail: olgasc@dep.uminho.pt

‡ e-mail: jmaia@dep.uminho.pt

polymer blending. The design of new polymer blends combining the characteristics of their constituents requires the control of the two-phase morphology, *i.e.*, the shape and size of the disperse particles. In the case of immiscibility of the blend components, the *in situ* generation of a compatibilizer *via* grafting or exchange reactions (during reactive extrusion) forming a block copolymer at the interface is a well known technique for producing a stable morphology with the adequate size of the disperse phase [1, 2].

Polymer blends can also be viewed as composites, since these are systems consisting of at least two materials with identifiable interfaces or interphases [3]. In practice, the disperse phase now consists of a fiber-type reinforcement, as the aim is to improve the mechanical performance of the matrix. Often, good adhesion between the fiber and the matrix can only be obtained if the former is coated with a coupling agent prior to the impregnation phase.

A new type of fiber polymer composites, designated as microfibrillar reinforced composites (MFC) was proposed by Fakirov and co-workers a few years ago [4–7]. These are developed from polymer blends and consist of microfibrils of flexible chains embedded in a matrix, which are created by orienting and annealing the blend below the melting temperature of its higher melting temperature component. Also, upon the annealing stage (denoted by Fakirov as isotropization step) chemical reactions (condensation and transreactions) in the melt and solid state can take place at the interface, yielding a co-polymer, *i.e.*, a self-compatibilization effect is produced [3].

The mechanical properties (in terms of tensile strength and tensile modulus) of MFCs are typically 30–50% higher than the values calculated from the rule of mixtures with the properties of the individual components [3, 8]. As anticipated, isotropization results in a slight decrease of the modulus and in a significant reduction of the strength when compared with the as drawn blends. On the other hand, the operating window for injection molding of the specimens must be defined carefully in order to preserve the fibrillar structure. The feasibility of the MFC approach has been tested with various polymer combinations, namely blends of poly(ethylene terephthalate), PET/polyethylene, PE, PET/polyamide 6, PA6, PET/polypropylene, PP, PA6/PP [3, 8–10], poly(buthylene), PBT/polyarylate, PAr [11], PA6/PA66 [12] and PP/PE [13].

Most of these blends were prepared in a single screw extruder and quenched in a water bath, followed by drawing in a tensile testing machine, chopped into pellets and subsequently injection molded (see, for example, [8] and [12]). Depending on the blend, isothermal annealing with fixed ends for several hours may be carried out before further processing [12].

Therefore, this work aims at preparing MFCs under conditions where scale-up to an industrial process can be foreseen. Blending PET with high density polyethylene, *i.e.*, blending a condensation polymer with a polyolefin, which exhibit clearly distinct melting points and are a priori immiscible, was carried out. For the purposes of process optimization and control it is also relevant to understand the evolution of the morphology of the composite along the process and correlate it with the thermomechanical history it was subjected to. Thus, blending was performed in a co-rotating twin screw extruder, which exhibits particularly good dispersion and heat transfer characteristics as well as good control of the residence time, fitted with a number of collecting devices that are able to remove quickly (within 2–3 seconds) a sample of material from inside the machine at a given location, which may be immediately quenched for subsequent characterization.

The linear viscoelastic response under small amplitude oscillations of liquid polymer blends has been correlated with morphology changes during processing. For example, an increase in elasticity and long time processes at low frequencies has consistently been reported and related to the deformation and recovery to the equilibrium shape of the disperse particles due to interfacial tension [14]. Covas *et al.* [15] monitored the rheological behavior of immiscible and reactive polymer blends along an extruder and correlated it with the morphological changes observed with electron microscopy. The dynamic viscosity and storage modulus decrease substantially upon melting of the components, and are further reduced along the barrel. This could be explained by changes in the disperse phase particle size, or by a competition between changes in particle size and interfacial structure, for immiscible and reactive blends, respectively, together with matrix degradation. In the present case, and due to the differences in the thermal properties of the two materials, a blend of a solid or highly viscous melt (PET) embedded in a liquid matrix (HDPE), rather than the more conventional blend of two polymers well above their melting

temperatures is to be prepared. Rheology should also be a powerful tool to complement the observations under the microscope.

## 2. EXPERIMENTAL

### 2.1. Materials

Commercial extrusion grades of a high density polyethylene, HDPE, HE8342 from Borealis, and a poly(ethylene terephthalate) Type D-405 from Trevira Fibras, S.A., with a melting range of 221 – 242°C, as determined by Differential Scanning Calorimetry, were selected for this work. PET was dried for 3 hours at 165°C before extrusion. HDPE/PET blends with a 70/30 weight ratio were prepared.

### 2.2. Production of the Composites

HDPE/PET blending was carried out in a Leistritz LSM 30.34 co-rotating intermeshing twin-screw extruder using the screw schematized in Figure 1 and described in Table I. The screw profile includes transport elements, two kneading blocks with staggering angles of  $-30^\circ$  (left-handed) and a left-handed transport element, and has been used frequently for melt blending purposes. The intensive mixing and heat transfer produced by the first kneading block causes material melting, while the second kneading block with an adjacent left element induces further mixing. Barrel temperatures were set at 220°C in the initial barrel sections and at 240°C in the rest of the barrel and die, in order to minimize the degradation of HDPE whilst attempting to melt the PET. The blends were produced at a flow rate of 2 kg/h (HDPE and PET were previously tumble mixed) as defined by a K-Tron Soder twin screw compact gravimetric feeder, using two different extruder screw speeds (40 and 100 rpm). It is anticipated that the shear rate level produced by the higher screw rotating frequency, coupled to the smearing effect of the kneading discs, will induce complete melting of PET.

Figure 1 also shows the location of a series of sampling devices that were inserted along the barrel at positions where the material should be subjected to more intensive thermomechanical stresses, *i.e.*, where

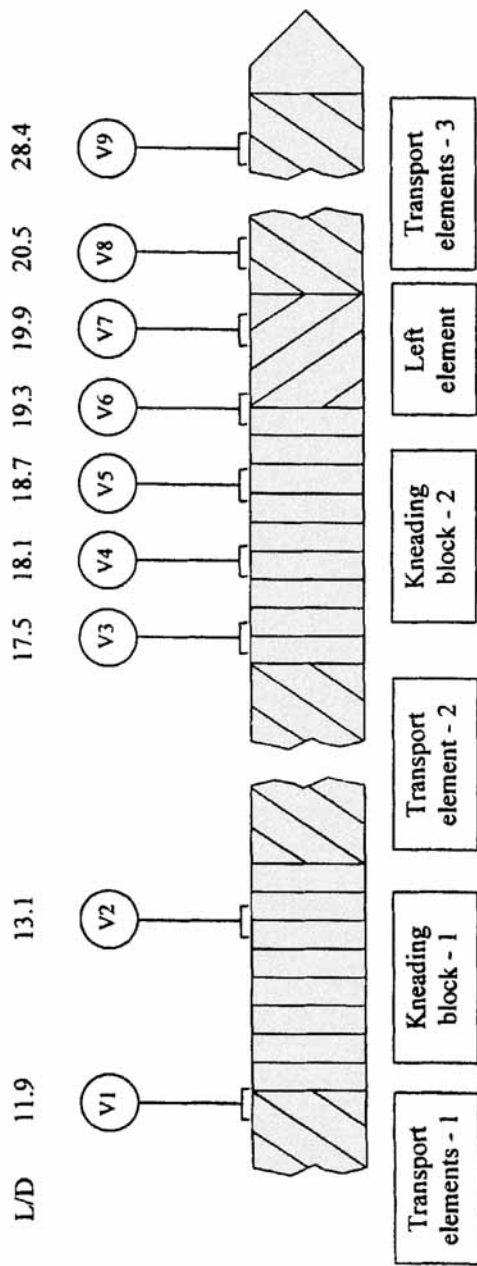


FIGURE 1 Extruder layout and location of the collecting devices (valves).

TABLE I Extruder: location of the collecting devices (valves)

<i>Description</i>	<i>Element code*</i>
Transport elements-1	60/120 + 45/120 + 30/120 + 30/30
Kneading block-1	8 – 30°
Transport element-2	30/120
Kneading block-2	9 – 30°
Left element	30/30
Transport elements-3	60/30 + 45/60 + 30/120 + 20/90

\* Transport elements – pitch (mm)/length (mm); kneading blocks – number of discs, staggering angle.

the most significant changes in morphology should occur. Circa 2 g of material could be removed within 2–3 seconds from the extruder, the samples being immediately quenched in liquid nitrogen in order to avoid further morphological changes. These tools and the corresponding experimental procedure were presented and validated elsewhere [16]. Measurement of the average material temperature was simply done by sticking a fast response thermocouple into the freshly collected material nut [17], the results being shown in Table II.

The extruder was coupled to a pelletizing die with two circular holes of 2 mm in diameter. Apart from the extruder/die combination and feeder, the extrusion line comprises a first water bath and haul-off unit, a second water bath and haul-off unit and a pelletizer downstream, as shown in Figure 2. The extrudate is initially cooled down and drawn with a draw ratio of 2 in order to stabilize both its cross-section and the line velocity. Drawing for the formation of a MFC is performed at the second stage, by setting the water in the bath at 94°C and the linear speeds of the two haul-off units in order to impose a

TABLE II Barrel/die set and average material temperatures at different locations

<i>Location</i>	<i>Set temperature</i> (°C)	<i>Material temperature (°C)</i>	
		<i>40 rpm</i>	<i>100 rpm</i>
V1	220	217.9	207.7
V2	220	236.7	249.7
V3	240	244.5	261.7
V4	240	243.4	265.4
V5	240	245.2	267.1
V6	240	245.6	268.9
V7	240	244.3	264.7
Die	240	–	–
Extrudate	–	248.3	254.0

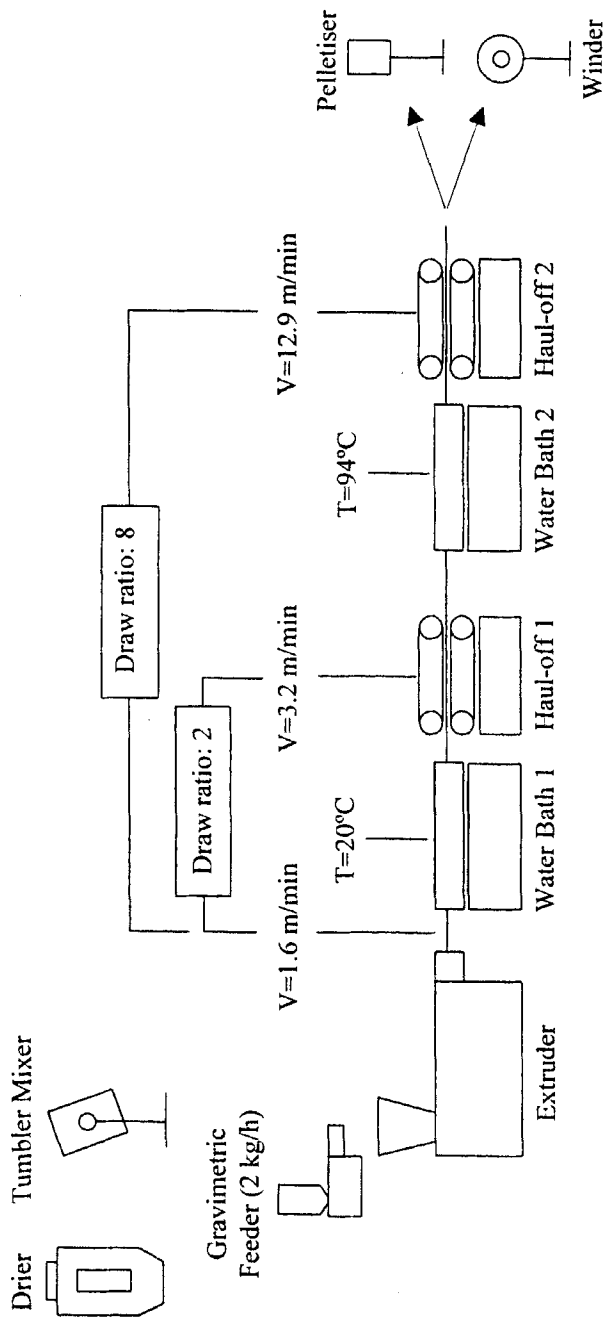


FIGURE 2 Materials preparation sequence and extrusion line used for the production of the MFC.

further draw ratio of 4. Therefore, since it emerges from the die, the extrudate is subjected to a total draw ratio of 8. Pellets about 4 mm long and 1 mm in diameter were produced, but bristles were also stored. Significant practical difficulties in achieving a good quality cut of the pellets were found.

### 2.3. Morphology

After fracture of the samples in liquid nitrogen and gold plating, the morphology of the blend was studied using a Leica S360 scanning electron microscope. For specific samples, etching with boiling xylene removed the polyolefin fraction; the PET residue was later observed under an Olympus BH-2 polarized light microscope.

### 2.4. Rheology

Isothermal frequency sweeps (from  $4 \times 10^{-3}$  to 40 Hz) at various temperatures were performed in a Reologica StressTech HR rotational rheometer, using 25 mm diameter parallel plates and a 1.1 mm gap. Stress sweep experiments were carried out at various constant frequencies, in order to ensure that the response of the material remained within the linear viscoelastic domain.

The nut-shaped samples collected from the twin screw extruder, or from several locations along the extrusion line, were compression molded for 10 min at 165°C under a pressure of 20 tons into discs 25 mm in diameter and 1.2 mm thick. As will be discussed later, the fibrillar structure was preserved under these conditions.

TABLE III Injection molding operating conditions

	<i>HDPE/PET</i>	<i>HDPE</i>
Injection temperature (°C)	165	165
Injection pressure (bar)	85	67
Injection speed (mm/s)	20	20
Injection time (s)	1.33	1.38
Screw speed (rpm)	150	150
Back pressure (bar)	2	2
Cooling time (s)	15	15
Mold temperature (°C)	40	40

## 2.5. Mechanical Properties

ASTM type 4 tensile test specimens were injection molded in a Klockner Ferromatik FM20 machine, using the operating conditions presented in Table III.

Tensile properties (modulus and stress and strain at yield and break) were measured at 23°C using an Instron 4505 universal testing machine with a 50 mm/min cross-head speed.

## 3. RESULTS AND DISCUSSION

### 3.1. Morphology Evolution

Previous studies on the evolution of various immiscible and reactive polymer blends along co-rotating twin screw extruders demonstrated that a dramatic decrease in the particle size of the disperse phase, from millimeter to micrometer scale, occurs in a very short axial length immediately after melting of the components, as a result of the interfacial area generated by the complex flow through the staggering kneading block [16, 18]. Further downstream, the rate of morphology evolution slows strongly, although a decrease in particle size distribution may still be significant.

It is generally recognized that rheological oscillatory tests preserve the morphology of immiscible polymer blends that is present before the measurements. A decrease of both the storage and loss moduli along the extruder has been reported, in parallel to the decrease in particle size and particle size distribution of the disperse phase. However, matrix degradation and flow induced orientation could also contribute to this decrease [15].

These conclusions were reached in the case where the processing temperature is well above that of melting of both individual components. In the present case, however, the operating temperature window is very narrow since one must ensure that HDPE does not degrade and also that PET is completely molten. Figure 3 shows the storage modulus,  $G'$ , of both materials at 245, 255 and 265°C. HDPE has a behavior typical of a viscoelastic melt throughout the whole temperature range analyzed, but PET only does so at 265°C, showing a distinct "solid-like" behavior at 245 and 255°C. Therefore, and given

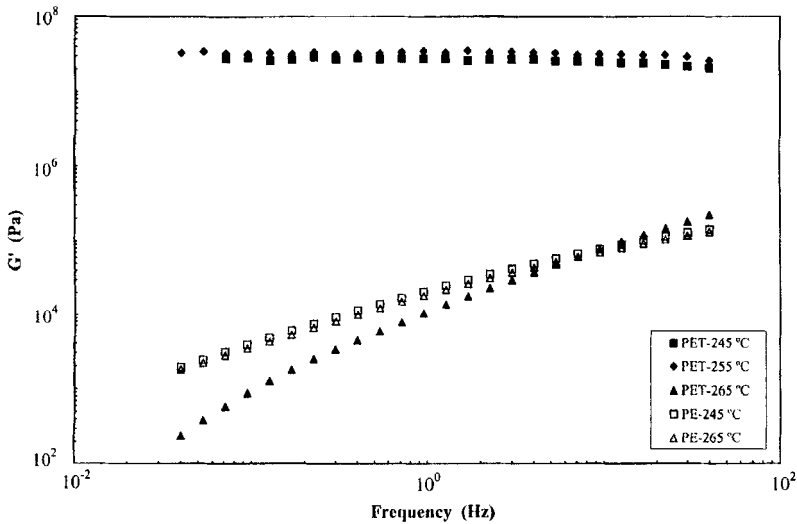


FIGURE 3 Rheological behavior (elasticity) of PET and HDPE at various temperatures.

the average temperatures reached by the blend at the various locations along the screw (presented in Tab. II), it is expected that when using a screw speed of 40 rpm PET will effectively behave as an elastic solid. This implies that its dispersion within HDPE will be accomplished essentially by the mechanical smearing of the pellets when flowing through the mixing sections. When the rotational speed of the screws is increased to 100 rpm, and again considering the temperature data shown in Table II, PET is already molten but still shows a high degree of elasticity, which means that it is able to endure high deformations and so its dispersion within the HDPE will be accomplished through its progressive breaking-up into smaller droplets, *i.e.*, it will occur through a viscoelastic droplet break-up type of mechanism (see, for example, [19]).

At 40 rpm no samples from the first kneading block (valves 1 and 2) were characterized because in the former the material is still solid and, in the latter, HDPE is already molten but PET is not, its granules still being visible to the naked eye. Also, no sample was collected just before the extrusion head (valve 9) since the pressure inside the extruder was not high enough to allow for quick sample removal. At 100 rpm, no samples from the beginning of the first kneading block

(valve 1) were studied, because the PET is still solid (much like in valve 2 at 40 rpm) and just before the extrusion head (valve 9), again due to the excessively low pressure at that point. Contrary to 40 rpm, samples could be collected at the end of the first kneading block, *i.e.*, in valve 2, since the higher the screw rotation speed, the larger the degree of viscous heating and the earlier in the barrel the material will melt.

Figure 4 depicts the evolution of elasticity (as measured by  $G'$ ) along the extruder with the screws rotating at 40 rpm. The results show that: i) the bulk behavior is indeed "solid-like", as can be seen from the small slope of the flow curves and ii) the response does not change significantly along the extruder, indicating that the morphology created upstream upon melting is being preserved to a large extent. The slight increase in elasticity is consistent with a possible growth in interfacial area resulting from the continuous mechanical smearing of PET. In this case, the work necessary to deform the highly elastic PET fragments (and consequently the elasticity) will also augment.

The morphological analysis performed using SEM corroborates this scenario. Figure 5 shows the SEM micrographs for locations along the extruder barrel corresponding to the beginning of the second kneading

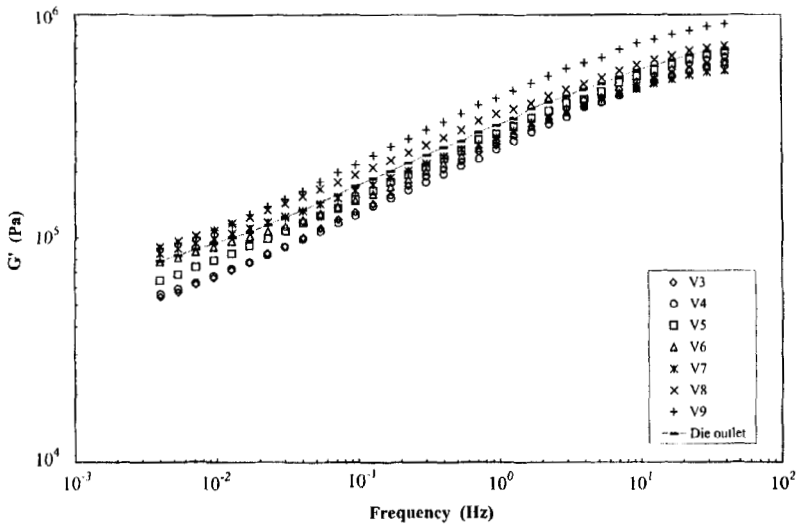


FIGURE 4  $G'$  dependency on frequency along the second mixing zone and at the die outlet (screw rotation speed of 40 rpm).

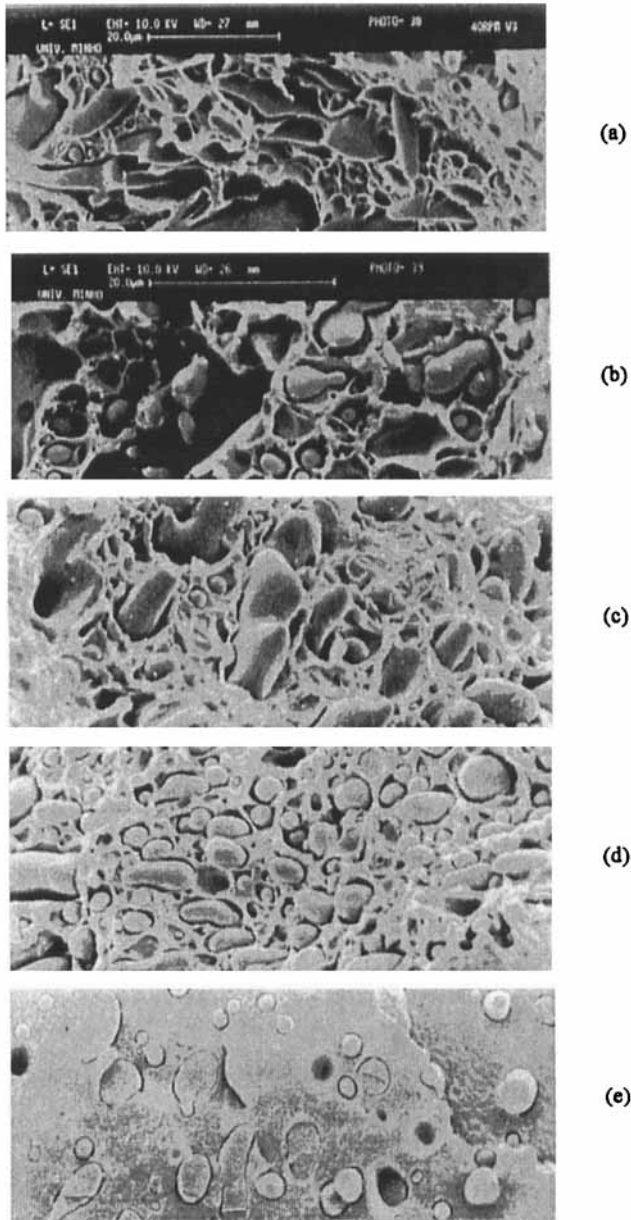


FIGURE 5 SEM micrographs of the morphological evolution along the second mixing zone and at the die outlet (screw rotation speed of 40 rpm): (a) valve 3; (b) valve 4; (c) valve 6; (d) valve 8; (e) die outlet.

block (valve 3, Fig. 5a), half way through it (valve 4, Fig. 5b), transition to the adjacent left element (valve 6, Fig. 5c), transition from the left element to the last transport section (valve 8, Fig. 5d) and, finally, die outlet (Fig. 5e). In valve 3 a relatively homogeneous PET dispersion is already apparent, although its smearing has just begun. The disperse particles width ranges typically from 4 to 6  $\mu\text{m}$  and their structure is elongated in the flow direction. The average particle width diminishes to approximately 3  $\mu\text{m}$  in valve 4 (probably the result of partial melting), but the dispersion does not seem to be significantly affected. This morphology survives mostly intact throughout the remainder of the kneading block, the left element and up to the extrudate, although a slight continuous reduction in particle size seems to occur. This reduction results in the anticipated increase in interfacial area with the consequences put forward earlier, namely in terms of an increase in elasticity, and validates the hypothesis regarding the dispersion mechanism at 40 rpm.

Figure 6 depicts the evolution of  $G'$  of the blend collected along the extruder when operating at 100 rpm. Figure 7 shows the changes along the extruder of both the storage and loss modulus, at a fixed frequency of 0.03 Hz. The results show that: (i) the blend behavior is less "solid-like" than previously at 40 rpm. This can clearly be asserted from the overall lower values of  $G'$  and the lack of the quasi-elastic plateau observed at 40 rpm; (ii) elasticity increases markedly as the material advances in the barrel, since  $G'$  becomes simultaneously higher and less dependent on frequency. Again, this behavior is consistent with an increase in interfacial area and, possibly, a progressively better dispersion; (iii) this marked increase in elasticity is accompanied by a less pronounced, but qualitatively similar increase in viscosity.

The morphological evolution, as assessed by SEM, confirms the assumption about the viscoelastic droplet break-up type of mechanism put forward earlier, as shown in Figure 8 for samples collected at the same points along the second mixing zone as in Figure 5. As already mentioned, melting occurs earlier in the extruder for 100 rpm than for 40 rpm and, as such, it is not surprising that the morphology observed in valve 2 at 100 rpm (Fig. 8a) is very similar to that observed in valve 3 at 40 rpm (Fig. 5a), *i.e.*, the material is seen to be already molten at the end of the first kneading block at 100 rpm and only at the beginning of the second at 40 rpm.

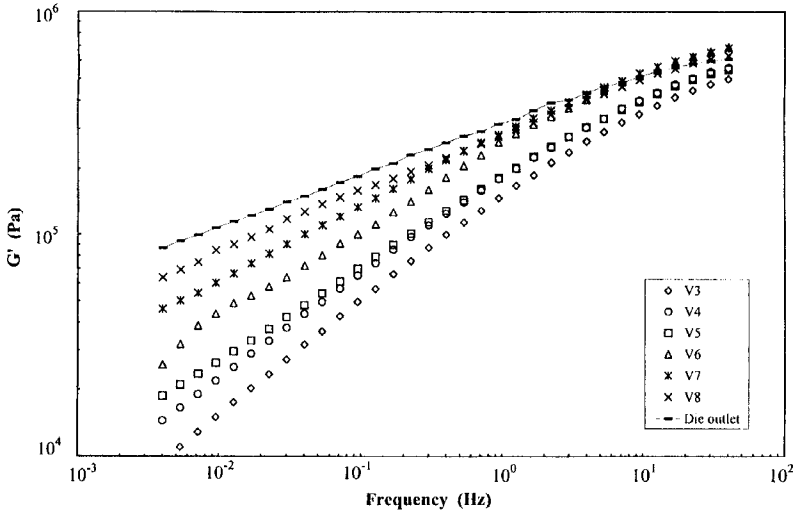


FIGURE 6  $G'$  dependency on frequency along the second mixing zone and at the die outlet (screw rotation speed of 100 rpm).

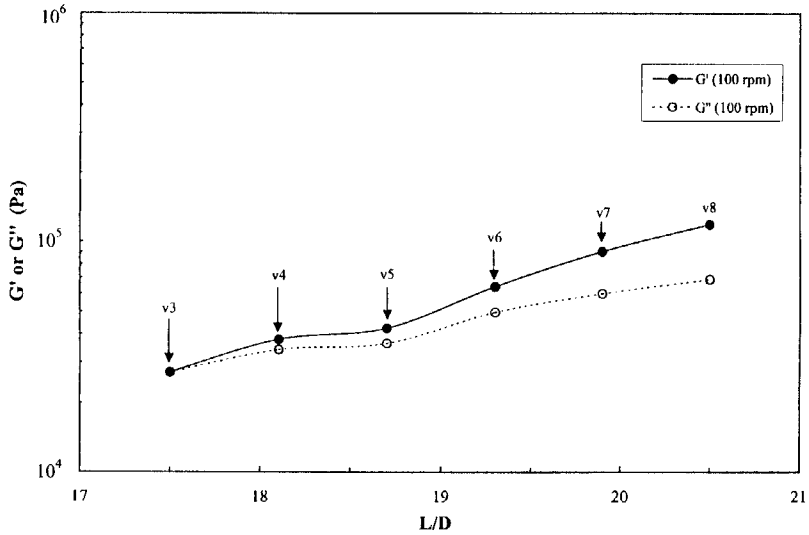


FIGURE 7 Evolution of the elastic and viscous responses at fixed frequency (0.03 Hz) for a screw rotation speed of 100 rpm.

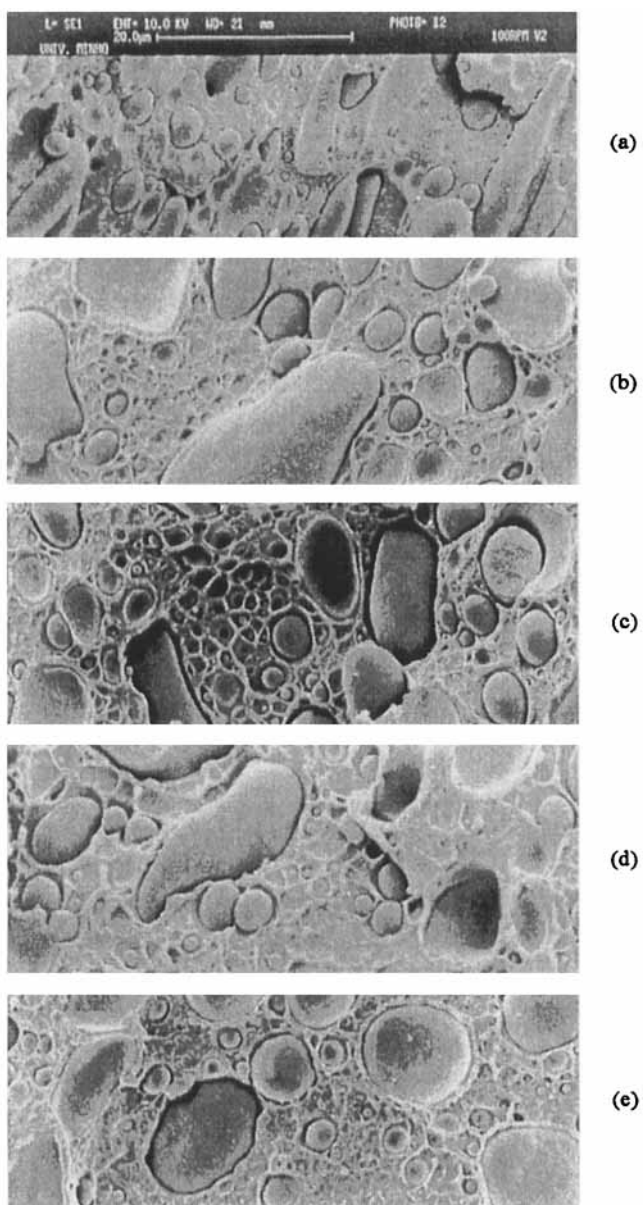


FIGURE 8 SEM micrographs of the morphological evolution along the first and second mixing zones (screw rotation speed of 100 rpm): (a) valve 2; (b) valve 3; (c) valve 4; (d) valve 6; (e) valve 8.

Apparently, there exists a bimodal distribution of PET particle sizes at 100 rpm (Figs. 8b through e) throughout the whole mixing section. As early as in valve 3, particles with approximately 1–2  $\mu\text{m}$  diameter coexist with others 30–40  $\mu\text{m}$  long and 5–10  $\mu\text{m}$  wide, that are generally aligned with the flow direction. The exception seems to be valve 8, but here the sampling time was longer due to the low pressure at the end of the left element, hence some elastic recovery of the large particles could have occurred. The number of smaller PET particles increases steadily along the mixing section, while the homogeneity of the dispersion also improves. This is consistent with larger droplets breaking-up progressively into smaller (typically by one order of magnitude) particles, as the former are subjected to a continuous shearing motion as the material advances along the mixing section. The main consequence of this breaking-up is a large increase in the total interfacial area, with the consequent increase in elasticity shown in Figure 7.

Figure 9 shows the evolution of both elastic and viscous responses (at a frequency of 0.03 Hz) along the extruder, from the beginning of the second mixing zone until the die exit, for both processing conditions. Two main features are apparent from this figure: (i) both the increase in elasticity and viscosity along the extruder are more pronounced for 100 rpm than for 40 rpm. This was expected since the interfacial area increases much more markedly at 100 rpm than at 40 rpm; (ii) both processing conditions seem to yield similar rheological responses of the extrudate, despite the fact that the morphologies are different (the morphology at 100 rpm is bimodal, with a high density of very small PET particles, whilst at 40 rpm it is unimodal but with a larger average particle size). Apparently, the higher degree of elasticity induced by the larger interfacial area of the (molten) PET droplets at 100 rpm is compensated by the higher elasticity of each (solid) PET particle at 40 rpm. However, since it was not possible to draw the blend processed at 40 rpm, in opposition to that processed at 100 rpm, this is an indication that drawability seems to be mainly sensitive to average particle size.

Figure 10 compares the elastic response of the extrudate at the die outlet, and after the first and second drawing stages, when a microfibrillar reinforced composite should have been formed. A large increase in elasticity is observed after the final drawing, which is

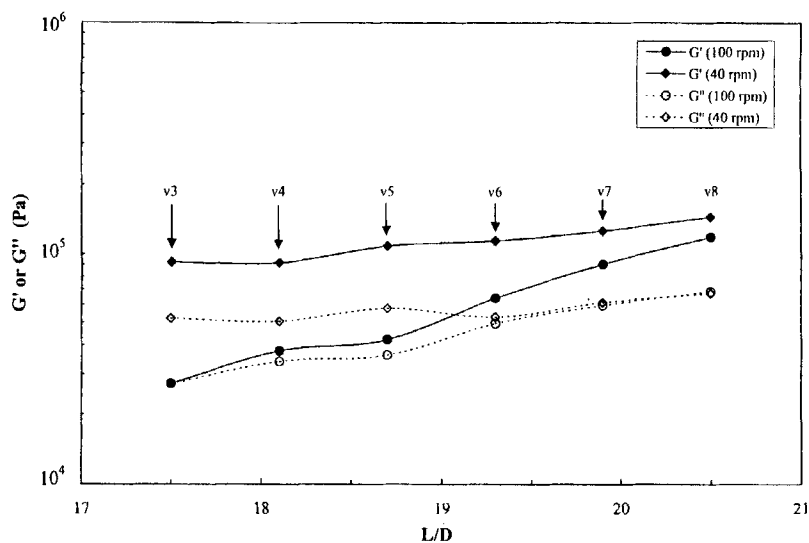


FIGURE 9 Evolution of the elastic and viscous responses at fixed frequency (0.03 Hz) for both screw rotation speeds.

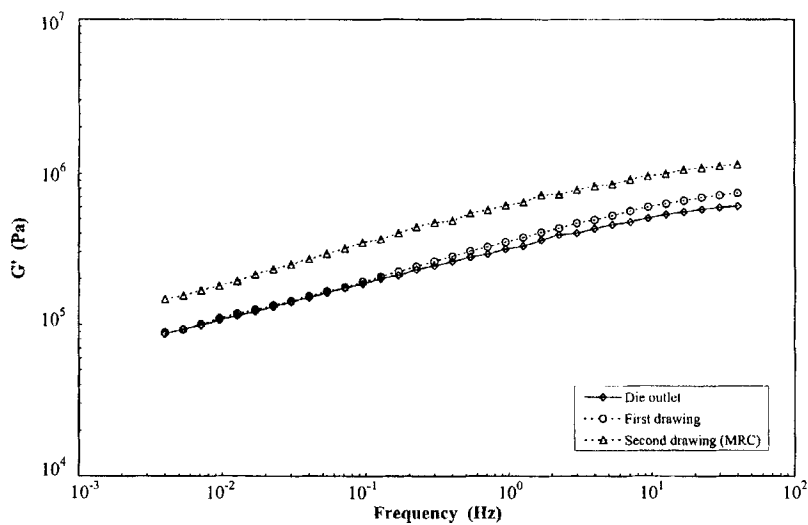


FIGURE 10 Elastic response at the die outlet and after the first and second drawing stages.

consistent with the morphology depicted in Figure 11, evidencing a highly oriented fibrillar structure. Figure 12 shows optical micrographs of the PET structure present after the two drawing stages, and dissolving the HDPE in xylene. Apparently, although a fibrillar structure is already obtained once the first drawing is completed, the uniaxial alignment is significantly improved and the cross-section is reduced upon further drawing.

### 3.2. Performance of the Blend

The evolution of the mechanical properties of the blend along the different processing stages, as extruded, drawn and injection molded is listed in Table IV, together with the properties of injection molded HDPE. Drawing improves significantly the mechanical performance of the blend, the modulus and stress at break increasing by over 300% and 400%, respectively. This result is encouraging since poor

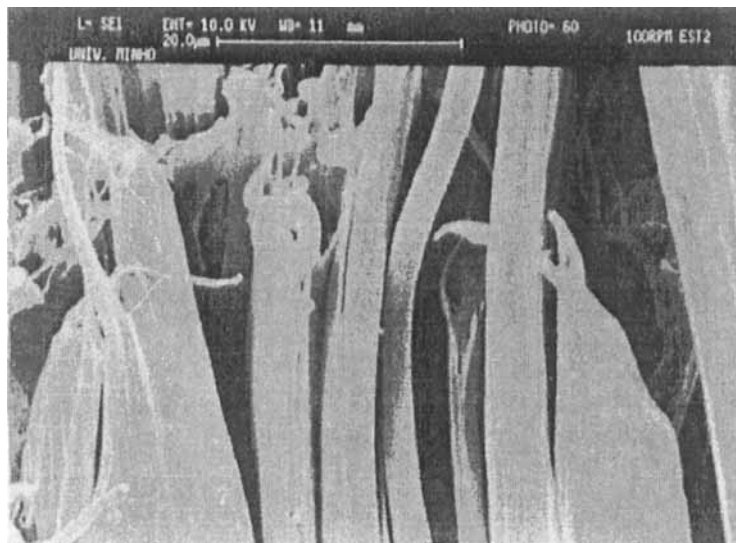


FIGURE 11 SEM micrograph of the drawn blend (MFC).

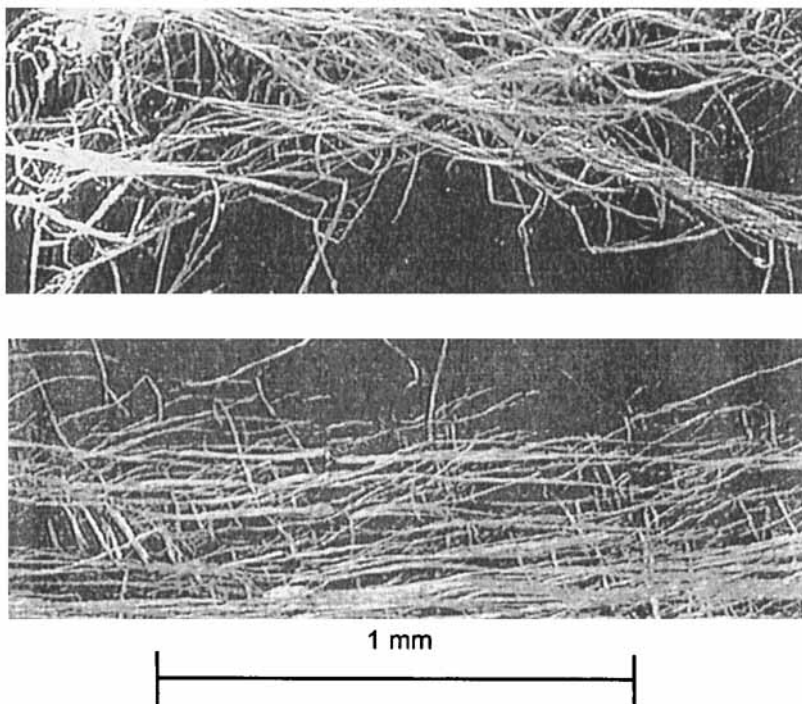


FIGURE 12 Optical micrograph of PET fibrils after the first (top) and second (bottom) drawing stages.

interfacial adhesion between the two components is evident from the SEM micrographs discussed earlier.

Injection molded drawn HDPE/PET specimens also show an improvement of around 50% in modulus and 140% in stress at break when compared with that of HDPE, but no improvement in modulus and only around 30% in stress at break over the extruded blend. This loss in mechanical performance is a direct consequence of the relaxation of the PET fibrils occurring during injection molding (see Fig. 13) despite the relatively low injection temperature (165°C). Confirmation of this comes from the fibrillar structure being retained after compression moulding at 165°C for the preparation of discs for rheometry, in which case there is no significant shear nor viscous dissipation (see Fig. 14).

TABLE IV Mechanical properties – average values (standard deviation between brackets)

	<i>Modulus</i> ( <i>MPa</i> )	<i>Stress at</i> <i>yield (MPa)</i>	<i>Strain at</i> <i>yield (%)</i>	<i>Stress at</i> <i>break (MPa)</i>	<i>Strain at</i> <i>break (%)</i>
As extruded HDPE/PET	1020 (64)	—	—	24.0 (0.9)	4.9 (0.6)
Drawn HDPE/PET	4145 (384)	147.1 (14.0)	21.1 (0.9)	127.5 (9.3)	80.4 (30.8)
Injected HDPE	660 (25)	36.4 (1.0)	17.4 (1.9)	13.1 (0.3)	22.4 (0.8)
Injected HDPE/PET	1016 (66)	—	—	31.8 (2.8)	9.5 (1.2)

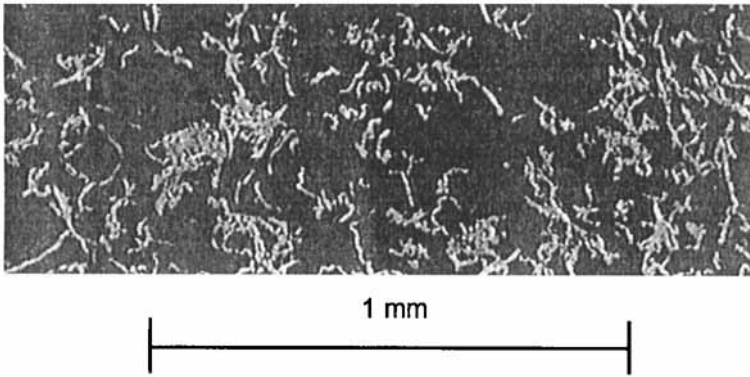


FIGURE 13 Optical micrograph of PET fibrils after injection molding.



FIGURE 14 SEM micrograph of the MFC after compression molding.

#### 4. CONCLUSIONS

Microfibrillar reinforced composites (MFC) based on blends of commercial HDPE and PET extrusion grades were prepared using

equipment and operating conditions relevant for direct scale-up to industrial practice. Although the polymers are immiscible and no compatibilization at the interphase was sought at this stage, the expected mechanical reinforcement capacity was observed.

The evolution of the blend morphology along the extruder can be correlated with changes in its viscoelastic response, namely the elastic modulus, which increases steadily as the mixing process develops. Blend drawability seems to be mainly dependent on the average particle size of the disperse phase.

Further work should concentrate on the optimization of processing, both in terms of screw geometry, processing window, post-extrusion conditions, as well as on the interphase compatibility.

### **Acknowledgements**

The authors are grateful to Prof. Stoyko Fakirov for enthusiastically introducing them to the topic and challenging them to produce MFCs under industrially relevant conditions. Trevira Fibras S.A. is gratefully acknowledged for supplying the PET for this study and Miss A. Nogueiro for carrying out some of the experiments.

### **References**

- [1] Utracki, L. A. (1990). *Polymer Alloys and Blends*, Hanser Publishers, New York.
- [2] Datta, S. and Lohse, D. (1996). *Polymeric Compatibilizers*, Hanser Publishers, New York.
- [3] Fakirov, S., Evstatiev, M. and Friedrich, K., In: *Polymer Blends*, Paul, D. R. and Bucknall, C. B. (Eds.), (John Wiley, New York, 2000), Chap. 33.
- [4] Evstatiev, M. and Fakirov, S. (1992). *Polymer*, **33**, 877.
- [5] Fakirov, S., Evstatiev, M. and Schultz, J. M. (1993). *Polymer*, **34**, 4669.
- [6] Fakirov, S., Evstatiev, M. and Petrovich, S. (1993). *Macromolecules*, **26**, 5219.
- [7] Fakirov, S. and Evstatiev, M. (1994). *Adv. Materials*, **6**, 395.
- [8] Evstatiev, M., Fakirov, S., Bechtold, G. and Friedrich, K. (2000). *Adv. Polym. Technol.*, **19**, 249.
- [9] Aharoni, S. M. (1997). *Intern. J. Polymeric. Mater.*, **38**, 173.
- [10] Evstatiev, M., Fakirov, S. and Friedrich, K., In: *Structure Development During Polymer Processing*, Cunha, A. M. and Fakirov, S. (Eds.), (Kluwer Acad. Publs., Dordrecht, 2000), p. 311.
- [11] Evstatiev, M., Krasteva, B., Oliveira, M. J., Serhatkulu, T. and Fakirov, S., *Intern. J. Polymeric Mater.*, in press.
- [12] Evstatiev, M., Schultz, J. M., Oliveira, M. J., Krasteva, B., Friedrich, K. and Fakirov, S. (2000). *Intern. J. Polymeric. Mater.*, **39**, 325.
- [13] Li, J.-X., Wu, J. and Chan, C.-M. (2000). *Polymer*, **41**, 6935.

- [14] Bousmina, M. and Muller, R. (1996). *Rheol. Acta*, **35**, 369.
- [15] Covas, J. A., Machado, A. V. and van Duin, M. (2000). *Adv. Polym. Technol.*, **19**, 260.
- [16] Machado, A. V., Covas, J. A. and van Duin, M. (1999). *J. Appl. Polym. Sci.*, **71**, 135.
- [17] Carneiro, O. S., Covas, J. A. and Vergnes, B. (2000). *J. Appl. Polym. Sci.*, **78**, 1419.
- [18] Sundararaj, U., Macosko, C. W., Nakayama, A. and Inoue, T. (1995). *Polym. Eng. Sci.*, **35**, 100.
- [19] Tanner, R. I. and Walters, K., *Rheological Phenomena in Focus* (Elsevier, Amsterdam, 1993), Chap. 6, pp. 129–149.